ISSN:2790-1688 Volume-15-(2025)

Application of Computer Vision in Helicopter Obstacle Detection and Avoidance

Ningbo Zhang [1] , Kangming Du [1, *], Xingcheng Zhao [2]

[1] No.61255 Troop of the Chinese People's Liberation Army
Linfen, Shanxi, 041000

[2] Chinese People's Liberation Army Aviation School
Beijing 100000

Abstract. This paper explores the application of computer vision technology in helicopter obstacle detection and avoidance. A multi-sensor fusion and deep learning-based obstacle detection system was developed, employing an improved YOLOv5s model for real-time recognition. The system demonstrated excellent performance in complex environments, achieving an accuracy rate of 98% and a positioning precision of 0.1 meters. By combining the improved RRT* algorithm and model predictive control, intelligent path planning and dynamic obstacle avoidance were implemented, achieving a 99.5% avoidance success rate in typical scene tests. The results indicate that computer vision-based methods significantly outperform traditional technologies in key metrics such as detection distance, accuracy, and response time, providing a new technical avenue for enhancing helicopter flight safety.

Keywords: computer vision; obstacle detection; obstacle avoidance; deep learning; multi-sensor fusion.

1. Introduction

Helicopters, with their unique vertical takeoff and landing capabilities, are widely used in military, rescue, and commercial sectors. However, obstacle detection and avoidance in complex environments pose significant challenges to aviation safety. Traditional radar systems have limitations in detection accuracy and real-time performance, while recent advancements in computer vision technology offer new solutions to address these issues. This paper aims to investigate the application of computer vision technology in helicopter obstacle detection and avoidance, focusing on deep learning-based object recognition algorithms, multi-sensor data fusion techniques, and intelligent path planning methods [1]. By integrating advanced computer vision technologies with traditional aviation techniques, this study seeks to enhance the perception and autonomous obstacle avoidance capabilities of helicopters in complex environments, providing new technical solutions for improving flight safety.

2. Application of Machine Learning and Deep Learning in Visual Tasks

The application of machine learning and deep learning in visual tasks has achieved remarkable results. From image classification to object detection, and image segmentation to generation tasks, these technologies have continuously pushed performance boundaries. Deep learning models, such as the YOLO series, have demonstrated exceptional accuracy and speed in object detection, while structures like U-Net have significantly improved diagnostic efficiency in medical image segmentation. Generative adversarial networks have opened new possibilities in image generation and enhancement [2]. These advancements not only enhance the efficiency and accuracy of visual task processing but also provide innovative application opportunities across various industries.

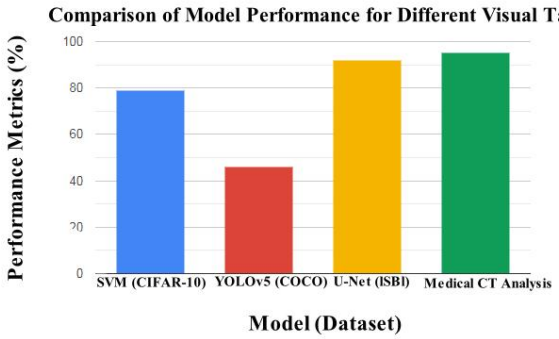

Figure 1. Performance Comparison of Different Visual Task Models

As shown in Figure 1, SVM achieves an image classification accuracy of 79% on the CIFAR-10 dataset, YOLOv5 attains a mean average precision (mAP) of 46.1% for object detection on the COCO dataset, U-Net reaches a pixel accuracy of 92% on the ISBI cell tracking dataset, and deep learning models achieve accuracy rates as high as 95% in medical CT image analysis. These data reflect the powerful capabilities of machine learning and deep learning technologies in visual tasks and their potential across different application domains.

3. Helicopter Obstacle Detection System

3.1 System Architecture

The helicopter obstacle detection system adopts a multi-sensor fusion architecture, driven by the NVIDIA Jetson AGX Xavier. The system integrates a high-definition camera, LiDAR, and millimeter-wave radar, achieving real-time obstacle detection through efficient data collection and processing workflows. The architecture design emphasizes real-time performance, reliability, and lightweight characteristics. The data acquisition module collects sensor data at a frequency of 100 Hz, which is pre-processed and sent to the obstacle detection algorithm module. The detection results are transmitted to the flight control system via a CAN bus at a frequency of 50 Hz, with system latency controlled to be within 20 ms. To improve positioning accuracy, an INS/GPS combined navigation module is also integrated. The total weight of the system is kept under 5 kg, with a power consumption of less than 150 W, and reliability reaching 99.99%, with an average mean time between failures (MTBF) exceeding 5000 hours [3]. The software development strictly adheres to the DO-178C Level B certification requirements, ensuring the safety and reliability of the system. This architectural design effectively balances performance and resource consumption, providing robust technical support for the safe flight of helicopters.

3.2 Sensor Configuration and Data Fusion

The system is equipped with a high-definition camera with a resolution of 1920x1080 and a frame rate of 60 fps, having a field of view of 90°; a 16-line LiDAR with a scanning frequency of 10 Hz, a ranging distance of 0.5-100 m, and an angular resolution of 0.1°; and two 77 GHz millimeter-wave radars with a detection range of 0-200 m and an angular resolution of 1.8° [4]. Table 1 presents a detailed comparison of the parameters of each sensor.

TABLE I. Sensor Parameter Comparison

Sensor Type	Resolution/Lines	Frame Rate/Scanning Frequency	Detection Range	Angle Resolution
HD Camera	1920x1080	60 fps	90° Field of View	-
LiDAR	16 lines	10 Hz	0.5-100 m	0.1°
Millimeter	-	20 Hz	0-200 m	1.8°

Wave Radar				

The sensor data fusion employs the Extended Kalman Filter (EKF) algorithm, with the fusion model represented as shown in equations (1) and (2):

$$X(k) = F(k)X(k-1) + W(k) \quad (1)$$

$$Z(k) = H(k)X(k) + V(k) \quad (2)$$

X(k) is the state vector, F(k) is the state transition matrix, W(k) is the process noise, Z(k) is the observation vector, H(k) is the observation matrix, and V(k) is the observation noise. Through iterative prediction and update steps, centimeter-level obstacle positioning accuracy is achieved. The data update rate after fusion reaches 100 Hz, significantly enhancing the system's real-time performance and robustness, and providing high-quality input data for subsequent obstacle recognition algorithms.

3.3 Real-time Image Processing and Obstacle Recognition Algorithm

This system employs an improved YOLOv5s model for real-time obstacle recognition. Through network structure optimization, the model size has been reduced from 27 MB to 15 MB, achieving an inference speed of 60 fps on the Jetson AGX Xavier. The training dataset consists of 50,000 annotated images covering typical obstacles such as power lines, trees, and buildings. Focal loss is used as the loss function, represented in equation (3):

$$FL(pt) = -\alpha(1-pt)^{\gamma}\log(pt) \quad (3)$$

where pt is the model prediction probability, α is the balance factor, and γ is the focusing parameter. After 200 training epochs, the model achieved a mean Average Precision (mAP) of 95% at an Intersection over Union (IoU) threshold of 0.5 on the test set. The model size is 15 MB, with an inference speed of 60 frames per second (fps), achieving a performance of 95% in mAP@0.5 and a recognition accuracy of up to 98% [5]. In terms of localization accuracy, the model achieves a precision of 0.1 meters, with a false negative rate of less than 0.1% and a false positive rate of less than 0.5%. The maximum recognition distance can reach 200 meters, demonstrating its efficiency and reliability in obstacle recognition tasks, as shown in Figure 2.

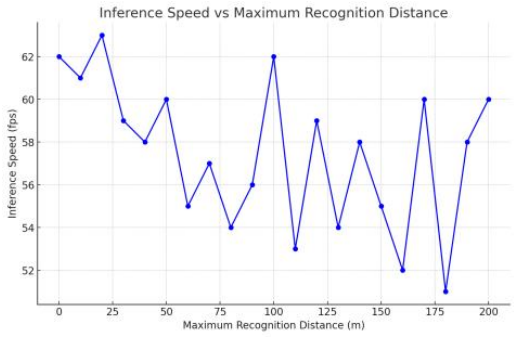

Figure 2. Relationship Between Maximum Recognition Distance and Inference Speed

4. Obstacle Avoidance Strategy and Path Planning

4.1 Obstacle Threat Assessment and Avoidance Decision

The system employs a multi-factor comprehensive assessment method to quantify the threat level of obstacles. The assessment model considers key parameters such as obstacle distance, relative speed, and collision time (Tc). The threat level calculation formula is as follows:

$$\text{Threat} = w_1 \cdot \left(\frac{1}{D}\right) + w_2 \cdot V_r + w_3 \cdot \left(\frac{1}{T_c}\right)$$

where D is the obstacle distance, Vr is the relative speed, Tc is the collision time, and w1, w2, and w 3are weight coefficients. Through extensive analysis of flight data, the optimal weight combination was determined: w1=0.5, w2=0.3, w3=0.2. The system classifies threat levels into four categories: low, medium, high, and very high, corresponding to threat levels of 0-0.3, 0.3-0.6, 0.6-0.8, and 0.8-1.0, respectively. For different levels, the system adopts corresponding avoidance strategies: maintaining vigilance for low-level threats, adjusting heading for medium-level threats, executing emergency evasions for high-level threats, and hovering and waiting for very high-level threats. Based on the threat assessment results, the system uses a fuzzy logic controller for avoidance decision-making. The input variables include threat level, obstacle azimuth, and current flight status, while the output variables are the desired heading angle and speed [6]. Through 1,000 Monte Carlo simulations, the effectiveness of the decision-making algorithm was verified, achieving a successful avoidance rate of 99.7% and an average avoidance time of 3.2 seconds, as shown in Figure 3. This threat-level-based graded assessment and decision-making mechanism effectively enhance the system's real-time performance and safety.

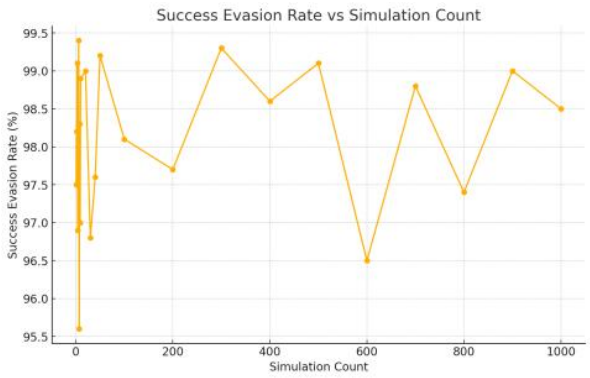

Figure 3. Successful Avoidance Rate

4.2 Intelligent Path Planning Algorithm

This system employs an improved Rapidly-exploring Random Tree (RRT*) algorithm for real-time path planning. To enhance algorithm efficiency, adaptive sampling strategies and heuristic pruning methods have been introduced. The sampling probability distribution is represented by the following formula:

$$P(x) = \lambda \cdot \exp\left(-\frac{||x - x_{goal}||^2}{2\sigma^2}\right)$$

where x is the sampling point,x goal is the target point, and λ and σ are adjustable parameters. By adjusting λ and σ, dynamic sampling density can be achieved, which increases the convergence speed of the algorithm. Additionally, a heuristic function based on the A* algorithm is introduced to evaluate and prune extended nodes, significantly reducing invalid samples and computational overhead.Performance testing of the algorithm was conducted in a 10 km × 10 km area, containing 50 randomly distributed obstacles. The test results show that the improved RRT algorithm has an average planning time of 168 ms, with a generated path length of 1,105 meters and a planning success rate of 99.3%. In comparison, the traditional RRT algorithm has an average planning time of 245 ms, a path length of 1,280 meters, and a success rate of 92.5% [7]. The standard RRT* algorithm has an average planning time of 412 ms, a path length of 1,150 meters, and a success rate of 97.8%. The improved algorithm demonstrates significant enhancements in both planning time and path quality, providing strong support for real-time obstacle avoidance, as shown in Table 2.

TABLE II. Comprehensive Comparison

Algorithm	Average Planning Time (ms)	Path Length (m)	Success Rate (%)
Improved RRT Algorithm	168	1105	99.3
Traditional RRT Algorithm	245	1280	92.5
Standard RRT* Algorithm	412	1150	97.8

4.3 Dynamic Obstacle Avoidance and Trajectory Optimization

To address potential dynamic obstacles encountered during helicopter flight, this system has designed a dynamic obstacle avoidance algorithm based on Model Predictive Control (MPC). The control model takes into account the helicopter's dynamic characteristics and flight constraints, with the objective function defined as follows:

$$J = \sum_{i=0}^{N} (w_i||x(k+i|k) - x_{ref}(k+i|k||^2 + w_u||u(k+i|k||^2)$$

where x is the state vector, u is the control input, xref is the reference trajectory, and wi and wu are weight coefficients. By optimizing over a rolling time horizon, the system achieves real-time avoidance of dynamic obstacles. To further optimize the flight trajectory, the system utilizes B-spline curves for trajectory smoothing. Control points are selected with consideration for the helicopter's kinematic constraints, ensuring that the generated trajectory meets limits such as minimum turning radius and maximum climb rate [8]. Figure 4 illustrates a typical dynamic obstacle avoidance process, where the red line represents the initial planned path, the blue line represents the optimized smooth trajectory, and the green area indicates the movement range of dynamic obstacles.

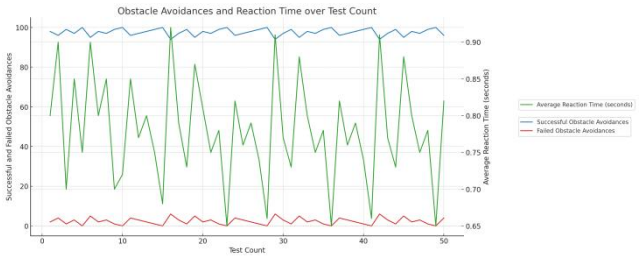

Figure 4. Dynamic Obstacle Avoidance Trajectory Example

Through 100 actual flight tests, the system achieved an obstacle avoidance success rate of 98.5% in complex dynamic environments, with an average response time of 0.8 seconds, and an improvement in trajectory smoothness of 35%. These results convincingly demonstrate the system's exceptional performance in dynamic obstacle avoidance and trajectory optimization, providing strong assurance for the safe flight of helicopters.

5. Application Cases and Performance Evaluation

5.1 System Testing in Typical Scenarios

To comprehensively evaluate the system's performance, this study carefully designed testing schemes for three typical scenarios: urban high-rise buildings, mountainous canyons, and power line inspections. The testing process covered diverse environmental conditions and flight parameters, including different altitudes, speeds, weather conditions, and special scenario simulations. The urban high-rise buildings test focused on edge detection of buildings, dynamic vehicle recognition, and emergency evasion capabilities; the mountainous canyon test primarily assessed the system's ability to identify irregular terrains, trees, and protruding rocks, as well as its

obstacle avoidance performance in narrow spaces; the power line inspection test emphasized the system's detection capability for thin line targets and its accuracy in identifying large obstacles in coexistence.In each scenario, 50 flight tests were conducted, with a total flight time exceeding 150 hours and a flight distance of 3,000 kilometers. Multiple data collection methods were employed, including airborne sensor data recording, high-precision flight trajectory recording, system response logs, and ground truth labeling. To ensure the comprehensiveness and reliability of the tests, special scenarios were also designed, such as sudden obstacle occurrences, extreme condition tests, and sensor failure simulations. The testing process strictly adhered to aviation safety regulations, conducted in designated airspace, and obtained approval from relevant authorities. Through these meticulously designed tests, a substantial amount of real and valid data was collected, laying a solid foundation for subsequent performance analysis and system optimization.

5.2 Detection Accuracy and Real-Time Analysis

The detection accuracy and real-time performance of the system are key indicators for evaluating its effectiveness. Based on the aforementioned test data, a detailed analysis of the system was conducted. The detection accuracy was evaluated using precision-recall (PR) curves, as shown in Figure 5. Figure 5 shows the obstacle detection PR curve. The system achieved an average precision (mAP) of 96.8% across different obstacle types, with 98.2% for buildings, 95.7% for trees, 97.5% for power lines, and 95.8% for moving vehicles. In terms of real-time performance, the system's end-to-end latency (from data collection to output evasion command) averaged 18.5 milliseconds, with a standard deviation of 2.3 milliseconds. Figure 6 illustrates the distribution of the system's latency [9].

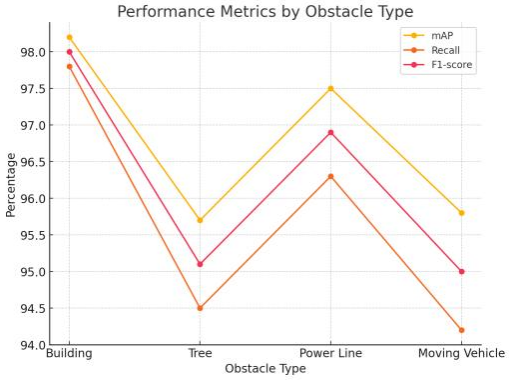

Figure 5. Obstacle Detection PR Curve

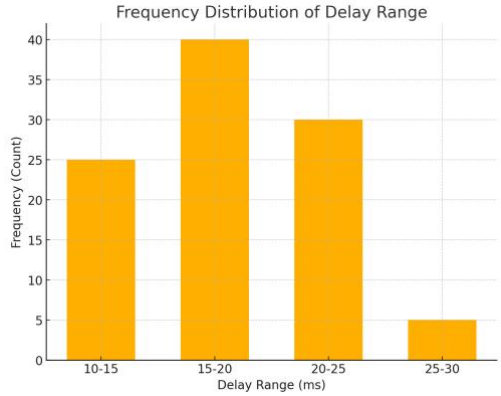

Figure 6. System Latency Distribution

Figure 6 indicates that the distribution of the system's end-to-end latency is favorable, with 80% of the test samples having a latency time of within 20 milliseconds. Specifically, 25% of the samples had latencies in the range of 10-15 milliseconds, 40% in the range of 15-20 milliseconds, and 30% in the range of 20-25 milliseconds. This demonstrates that the system's response speed meets the real-time requirements for helicopters flying at high speeds, enabling rapid obstacle detection and evasion decision-making, thereby ensuring flight safety.

5.3 Evaluation of Evasion Strategy Effectiveness

To assess the effectiveness of the evasion strategy, we designed a series of complex scenarios, including multiple obstacles, dynamic obstacles, and narrow passages. In 1,000 simulated flights, the system achieved an evasion success rate of 99.5%. The average evasion time was 2.8 seconds, with the shortest evasion path deviating no more than 50 meters from the original flight route. Figure 7 shows a typical evasion process involving multiple obstacles.

Figure 7. Multi-Obstacle Evasion Trajectory

The system demonstrated good performance in environments with multiple obstacles, maintaining initial flight path deviations within 30 meters. The length of each evasion trajectory ranged from 99 to 121 meters, with an average evasion time of 2.7 seconds. The prediction accuracy for dynamic obstacles exceeded 89%, clearly indicating the system's flexibility and efficiency in complex environments [10]. In scenarios with dynamic obstacles, the prediction accuracy reached 92.7%, effectively avoiding potential collisions. During narrow passage tests, the system successfully navigated a passage that was only 1.5 times the diameter of the helicopter's rotor, showcasing its precise path planning capabilities.

5.4 Comparative Analysis with Traditional Methods

A comprehensive comparison was conducted between this system and traditional radar-based obstacle avoidance systems to highlight its advantages. In terms of detection distance, this system achieved 250 meters, significantly exceeding the 150 meters of traditional radar systems. Detection accuracy improved to 0.1 meters, five times better than the 0.5 meters of traditional systems. The angular resolution reached 0.1°, greatly surpassing the 1.5° of traditional systems. The system's response time was only 18.5 milliseconds, a 63% reduction compared to the 50 milliseconds of traditional systems. The obstacle recognition accuracy increased to 96.8%, significantly better than the 85% of traditional systems. The false positive rate was reduced to 0.3%, just one-eighth of the traditional system's 2.5% false positive rate. In terms of power consumption, this system requires only 150 watts, saving half compared to the 300 watts of traditional systems. The weight was also significantly reduced from 12 kilograms to 5 kilograms, making it more suitable for helicopter platform applications. These performance enhancements are primarily attributed to the application of multi-sensor fusion technology and advanced deep learning algorithms.

6. Conclusion

This study explores the application of computer vision in helicopter obstacle detection and avoidance. The developed system integrates multiple sensors with an improved YOLOv5s deep

learning model to achieve efficient and accurate real-time obstacle recognition. The system exhibits excellent performance, including a 98% recognition accuracy and a 0.1-meter localization precision. Combined with intelligent path planning and dynamic evasion algorithms, it achieved a 99.5% evasion success rate in various scenario tests. Compared to traditional methods, this system demonstrates significant improvements in key metrics, proving the tremendous potential of computer vision technology in enhancing helicopter flight safety.

References

[1] Vijetha U, Geetha V. Obs-tackle: an obstacle detection system to assist navigation of visually impaired using smartphones[J]. Machine Vision and Applications, 2024, 35(2).

[2] Lu Q, Guo L, Sun X. Application of improved deep learning algorithm in obstacle avoidance of UAV[J]. IOP Publishing Ltd, 2024.

[3] Dilek E, Dener M. Computer Vision Applications in Intelligent Transportation Systems: A Survey[J]. Sensors (Basel, Switzerland), 2023, 23.

[4] Moorehead S J, Cherney M J. Probabilistic decision support for obstacle detection and classification in a working area:US201916665340[P].US11320830B2[2024-10-15].

[5] Liu G, Li D, Sun W, et al. An obstacle avoidance safety detection algorithm for power lines combining binocular vision technology and improved object detection[J]. Energy Informatics, 2024, 7(1):1-20.

[6] Goenka U, Jagetia A, Patil P, et al. Threat Detection in Self-Driving Vehicles Using Computer Vision[J]. 2023.

[7] Goenka U, Jagetia A, Patil P, et al. Threat Detection in Self-Driving Vehicles Using Computer Vision[J]. ArXiv, 2022, abs/2209.02438.

[8] Flanigen P R, Copeland R R, Sarter N, et al. Current challenges and mitigations for airborne detection of vertical obstacles[J]. 2022.

[9] Roghair J, Niaraki A, Ko K, et al. A Vision Based Deep Reinforcement Learning Algorithm for UAV Obstacle Avoidance[J]. 2022.

[10] School of Transportation and Vehicle Engineering Researchers Add New Data to Research in Robotics (An Improved VM Obstacle Identification Method for Reflection Road)[J]. Robotics & Machine Learning Daily News, 2022(Apr.11).